XL CILAMCE
IBERO-LATIN AMERICAN CONGRESS ON COMPUTATIONAL METHODS IN ENGINEERING
NOVEMBER 11-14, 2019
Praiamar Natal Hotel & Convention
Natal, RN-BRAZIL

THERMODYNAMIC FORMULATION OF CORROSION-CRACKING COUPLING IN REINFORCED CONCRETE FRAMES

C. A. C. Brant
J. Flórez-López
betocbrant@hotmail.com
julio.lopez@unila.edu.br
Federal University of Latin American Integration
Avenida Tancredo Neves, 6731, Zip-Code 2044 - CEP 85.867-970, Paraná/Foz do Iguaçu, Brazil

Abstract. The objective of this work is to propose a mathematical model for the coupling of corrosion, cracking and plasticity in the analysis of reinforced concrete structures. The corrosion phenomenon is considered due to chloride ions in the concrete that causes the reduction of the cross section of the steel bars and the penalization of the yield stress. The modeling of structural behavior is based on lumped damage mechanics and the laws of the thermodynamics of solids. The model proposed in this work is called elastoplastic with linear kinematic hardening, damage and corrosion; its internal variables are plastic rotation, damage level and corrosion level. The proposed model was used for the simulation of a reinforced concrete slab. In the simulation, the model represents the increase of the corrosion resulting from increments of cracking. Accelerating the corrosive process, damage evolution causes the reduction of the corrosion time for the appearance of the first plastic hinge.

Keywords: Corrosion by chloride ions, Damage mechanics, Plastic hinge, Reinforced concrete frames, Thermodynamics of solids.

1 Introduction

Corrosion is one of the most common forms of degradation of material properties due to interaction with the environment. Inevitably, this deterioration can occur in several types of materials, as in polymeric insulation present in the spinning of aging aircraft or even in selective-dissecting ceramics. However, corrosion is mainly associated with metallic materials. According to Shaw and Kelly [1], Koch (2002) shows that in the United States roughly US$ 276 billion per year is required to cover corrosion processes, focusing mainly on maintenance of utilities, transportation and infrastructure.

For Shaw and Kelly [1], as well as death and taxes, the corrosion of materials is something that must be avoided, and for this, it is necessary to understand how to deal with this phenomenon. For these authors, the fundamental cause of all corrosion is the Gibbs free energy variation of the analyzed system. In this sense, the production of the metal alloys involves the addition of energy to the system, so that as a result of the thermodynamic struggle, over time, the metal is naturally driven to return to its more stable state (low energy oxide). This process of returning to the oxide form is called corrosion, and although it is natural, there are control methods that can be used in its prevention, such as: application of protective coatings that act as a barrier or protection of sacrifice; additions of chemical species to the environment to inhibit corrosion; altering the chemistry of the alloy to make it more resistant to the phenomenon; and treating the metal surface to increase its corrosion resistance. Thus, it is worth noting that the corrosion rate is a subject of interest in many researches, and it is controlled by the nature of the surface of the metal and the nature of the environment in which it is found, or by the combination of both.

Still, according to Shaw and Kelly [1], as infrastructures of industrialized countries grow older,

more failures due to corrosion are expected to occur. The replacement of all bridges and pipelines, for example, would obviously be expensive and unnecessary, since it is understood that most of these infrastructures may still be in good working order. The challenge of finding out which ones are failing and how long they can last is the function of predicting the useful life. This area involves work with computer researchers, civil engineers, mechanics, chemists, electrical, information and economists.

Thus, this work enters into the subject of corrosion-cracking coupling in reinforced concrete structures, since in the perspective of civil engineering and structures, concrete undoubtedly stands as one of the most used materials in the world.

The importance of this cementitious material is known for the characteristic properties, such as significant mechanical resistance, durability, ease of molding and fire resistance, which potentiate its demand in several applications within civil construction. In this sense, basically composed of the water, cement and aggregates mixture, the hardened concrete can achieve significant compressive strength, around 32 MPa after 28 days of curing (common concrete in Brazil). However, this material does not have a large capacity to withstand tensile stresses, being restricted to approximately 1/10 of the compressive strength. But, because the stresses are mixed between compression and traction, in structures of current constructions, it is sought to associate the concrete with another material that has good tensile strength, the steel reinforcement is the most usual, being arranged longitudinally in the regions of traction of the part, thus giving rise to a composite material called reinforced concrete (ARAÚJO [2]; CARVALHO and FIGUEIREDO FILHO [3]).

As a joint work, the concrete-reinforcing bond strengths ensure that the tractional steel bars work only with the deformation effect of the concrete surrounding them. Thus, even if the structure possesses deformed regions capable of cracking the concrete, it will be able to ensure adequate resistance to the calculation request, thanks to the steel. In addition, the concrete wrapped in the reinforcements, besides having the function of adhesion, also serves to protect the steel bars against corrosion. In this sense, Araújo [2] states that cracking of concrete is inevitable in economic structures of reinforced concrete, this would facilitate the discovery of steel and, consequently, the propagation of corrosion, but the durability of the part is not necessarily impaired when the minimum covering limit is respected in the structural calculation. This limit depends on the aggressiveness of the external environment in which the structure is located.

However, it is known that reinforced concrete structures deteriorate over time due to mechanical, chemical and environmental effects. For Bertolini et al. [4] and Carsana et al. [5], one of the major concerns regarding long-term performance and structural durability is related to the corrosion effects of steel embedded in concrete, which is usually initiated by the disassembling of the reinforcement through carbonation reactions and/or ions chlorides adducts from the external medium.

Gentil [6] explains the corrosion as the spontaneous deterioration of a material, especially the metallic ones, by the chemical or electrochemical action of the environment, being able to be allied to the mechanical efforts. This phenomenon causes structural changes, chemical variations and wear on the surface of the steel reinforcement, which can make them unviable to the originally assigned use.

The process of destabilizing the concrete passivating layer around the steel reinforcement is considered the initial phase of corrosion. Then, the formation of a cell of corrosion occurs that is responsible for the propagation of this phenomenon (FIGUEIREDO and MEIRA [7]).

In this context, because it is a probabilistic phenomenon that depends on environmental factors, structural characteristics and time exposed, the structural analysis that contemplates the corrosion of the reinforcement is linked to high complexity in simulations. However, through the theoretical basis offered by thermodynamics of solids and frames, it is foreseen the possibility of making a mechanical model of analysis of reinforced concrete structures that take into account the corrosion of the reinforcement.

Coelho [8] pioneered the analysis of corrosion-cracking behavior in reinforced concrete structures through the lumped damage mechanics. As a result, the author obtained that the increase of the corrosion rate generates reduction of the cross section of the reinforcement and the penalization of the yield function, causing that there is loss of rigidity and of resistant capacity, favoring increases of deformations and of cracking in the structure.

Coelho [8] concludes that the theory of lumped damage allows the direct and efficient coupling of

corrosion in inelastic analyzes, through the definition of a corrosion state variable. The model could be modified to contemplate several laws of evolution of corrosion, which are parameters of the start time and the corrosion rate of the reinforcement. In addition, due to the low computational cost associated with lumped damage theory, probabilistic structural analyzes were feasible through the Monte Carlo simulation method, proving that this theory and probabilistic analysis can work well together.

Finally, Coelho's [8] conclusion on reliability analysis is the possibility of determining the failure path of the structure. Redistribution of internal stresses is directly related to the corrosive process, and it is possible to have unexpected collapse mechanisms - a change in the critical path of hyperstatic structures - and this is an important point to define possible repairs to structures under corrosion.

In the study done by Dahmer [9], the thermodynamics of solids is used to develop the thermodynamics of frames. Thus, the author validates the thermodynamics of frames with auxiliary models consolidated in the literature: perfect elastoplastic model, elastoplastic model with linear kinematic hardening, elastic model with damage, elastoplastic model with linear kinematic hardening and damage. Through the development of this thermodynamics, the author performs the structural analysis of a grid considering the evolution of pit corrosion.

However, the work of Coelho [8] and Dahmer [9] did not consider the evolution of corrosion caused by the propagation of cracking in reinforced concrete structures. Thus, for these authors, the advance of the corrosion of the reinforcement is due exclusively to chemical forces, section properties and concrete properties.

In this sense, the present research proposes to study the coupling of the reinforcement corrosion in the structural analysis, through the lumped damage mechanics. The objective of this work is to develop a mathematical model for the coupling of corrosion by the effect of chloride ions, cracking and plasticity in the analysis of reinforced concrete structures, as well as to provide the choice of any model of pitting corrosion in the literature for analysis of complex structures subject to chemical and mechanical loading. The lumped damage mechanics is based on fracture mechanics and classical damage theory, and are therefore chosen because of their relative simplicity and significant theoretical consistency (FLÓREZ-LÓPEZ, MARANTE and PICÓN [10]).

As novelties of this research, we intend to collaborate with the studies on the development of the thermodynamics applied to frames (thermodynamics of frames) and, besides considering the evolution of the corrosion in the structural analysis, to contemplate the influence of the part of the corrosion due to the cracking of the concrete.

2 A model coupling cracking, plasticity and corrosion

This model, besides containing the plastic deformations $\{\Phi^p\}$ and the cracking of the concrete $\{D\}$, also takes as internal variable the corrosion of the reinforcement by pits $\{C\}$. These variables are applied to the inelastic hinges as shown in Figure 1.

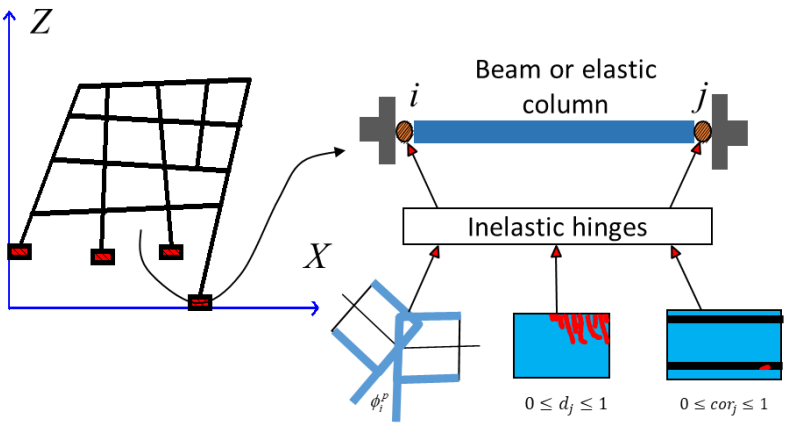

Figure 1. Internal variables of the elastoplastic model with linear kinematic hardening, damage and corrosion

As hypothesis for the development of this model, it is assumed that pitting corrosion occurs in the hinges (i and j), where the requests for bending moments are larger.

$$\{C\}^t = (c_i, c_j) \tag{1}$$

The level of corrosion (cor or c_i for any node i) is defined by Equation 2.

$$cor = \frac{A_{cor}}{A_0} = 1 - \frac{A_{ef}}{A_0} \tag{2}$$

In which A_{cor} is the corroded steel area and A_0 is the original steel area of the cross section of the reinforcement under analysis.

Thus, the variables c_i and c_j represent the corrosion levels of the reinforcement in the respective hinge and assume values between 0 and 1, such that the closer to 1, the more the steel bar will be corroded in that position of the structure.

The corrosion caused by chloride ions depends on the depth of the pit (p), which in turn is associated with the environmental conditions, the cover of the reinforcement, the properties of the concrete, the time of beginning of the corrosion and the time elapsed after the beginning of the corrosion. Thus, the corrosion evolution function (O) can be written as a function of the chemical generating forces (CF), concrete properties (CP) and section properties (SP), according to Equation 3.

$$O = O(CF, CP, SP) \tag{3}$$

The thermodynamic potential representing this model is in the form of a function G_b=$G_b(\{M\},\{\Phi^p\},\{D\},\{C\})$, and is represented by Equation 4.

$$G_b = \frac{1}{2}\{M\}^t[F(D)]\{M\} + \{M\}^t\{\phi^p\} - \frac{1}{2}\{\phi^p\}^t[H(D,C)]\{\phi^p\} - I(D,C) + \frac{\{O\}^t\{C\}}{\xi} \tag{4}$$

It is worth mentioning that ξ is a constant to be established experimentally and is defined by the inverse of the unit of energy.

The function that represents the resistance gain associated with the cracking process ($I(D,C)$) depends on the parameters $q(c_i)$ and $q(c_j)$, which are now in function of the corrosion levels (c_i and c_j), according to Equation 5. The parameters q are necessary for the analysis of the lumped damage mechanics (FLÓREZ-LÓPEZ, MARANTE and PICÓN [10]).

$$I(D,C) = -\frac{1}{2}q(c_i)ln^2(1-d_i) - \frac{1}{2}q(c_j)ln^2(1-d_j) \tag{5}$$

The hardening of the reinforced that now considers the damage and corrosion ($[H(D,C)]$) is given by Equation 6. In this equation, the parameters $h_i(c_i)$ and $h_j(c_i)$ are in function of the levels of corrosion (c_i and c_j), where the parameters h were reviewed in the work of Flórez-López et al [10].

$$[H(D,C)] = \begin{bmatrix} (1-d_i)h_i(c_i) & 0 & 0 \\ 0 & (1-d_j)h_j(c_j) & 0 \\ 0 & 0 & 0 \end{bmatrix} \tag{6}$$

By deriving the potential (Equation 4) in relation to the moment the associated elasticity law is obtained (Equation 7).

$$\left\{\frac{\partial G_b}{\partial M}\right\} = [F(D)]\{M\} + \{\Phi^p\} = \{\Phi\} \tag{7}$$

The derivative of Equation 4 in relation to plastic deformations determines the thermodynamic force related to plasticity $\{A\}$, which is associated with the yield function (Equation 8).

$$\{A\} = \left\{\frac{\partial G_b}{\partial \Phi^p}\right\} = \{M\} - [H(D,C)]\{\Phi^p\} \tag{8}$$

In addition, deriving Equation 4 in relation to the damage obtains the thermodynamic force related to the cracking $\{Y\}$ (Equation 9).

$$\{Y\} = \left\{\frac{\partial G_b}{\partial d}\right\} = \begin{Bmatrix} \frac{1}{2}\frac{Lm_i^2}{3EI(1-d_i)^2} - q(c_i)\frac{\ln(1-d_i)}{(1-d_i)} + \frac{1}{2}h(c_i)\left(\phi_i^p\right)^2 \\ \frac{1}{2}\frac{Lm_j^2}{3EI\left(1-d_j\right)^2} - q(c_j)\frac{\ln\left(1-d_j\right)}{\left(1-d_j\right)} + \frac{1}{2}h(c_j)\left(\phi_j^p\right)^2 \end{Bmatrix} \tag{9}$$

Finally, deriving the equation 4 in relation to corrosion obtain the thermodynamic force related to corrosion, denominated by the matrix $\{B\}$ (Equation 10).

$$\{B\} = \left\{\frac{\partial G_b}{\partial cor}\right\} = -\frac{1}{2}\{\Phi^p\}^t\left[\frac{\partial H(D,C)}{\partial cor}\right]\{\Phi^p\} - \left\{\frac{\partial I}{\partial cor}\right\} + \frac{\{O\}}{\xi} \tag{10}$$

The portion of the thermodynamic force of the corrosion linked to the plastic deformations was strategically neglected for the development of the study, resulting in Equation 11.

$$\{B\} = \left\{\frac{\partial G_b}{\partial cor}\right\} = -\left\{\frac{\partial I}{\partial cor}\right\} + \frac{\{O\}}{\xi} \tag{11}$$

Therefore, the law of evolution of corrosion obtained in this work is represented below, through Equation 12.

$$\{\dot{C}\} = -\xi\left\{\frac{\partial I}{\partial cor}\right\} + \{O\} \tag{12}$$

In this development, therefore, to complete the law of evolution it is necessary to determine the value of the constant ξ, which depends essentially on experimental results. For ξ = 0, it is assumed that the corrosion evolution law does not depend on the damage and will be equivalent to any of the results given by the models reviewed in literature (represented by the O function): model of Yalcyn and Ergun (1996), model of Liu and Weyers (1998) , model of Vu and Stewart (2000) and model of Martinez and Andrade (2009).

For this work, the O function was adopted as the corrosion rate evolution model proposed by Vu and Stewart [11] and the calculation of pit depth and effective area of corroded steel bars as developed by Stewart [12].

3 Numerical example

3.1 Modeling of behavior moment by curvature

The objective of this section is to represent the moment by curvature behavior of reinforced concrete beams (or slabs) subject to mechanical loading and pit corrosion effects. In turn, these effects considered are the loss of the effective area and the penalization of the tension of the steel reinforcements. For this, the experimental works of Du et al. [13] and of Kearsley and Joyce [14] were considered.

At first, we attempted to represent the behavior of experimental moment by curvature graphs obtained by Kearsley and Joyce [14]. The Figure 2 shows the structure to be studied (simply supported beam), 1.70 m long and 35 cm (base) by 13 cm (height) cross-section. The longitudinal tensile reinforcement is composed of 3 bars with 10 mm in diameter, and the longitudinal compression reinforcement, by a bar of 6 mm in diameter. The covering adopted by Kearsley and Joyce [14] was 2 cm and there were no transverse reinforcements. The two forces (P) cause the maximum bending moment to occur in the central section of the beam and without the influence of shear forces.

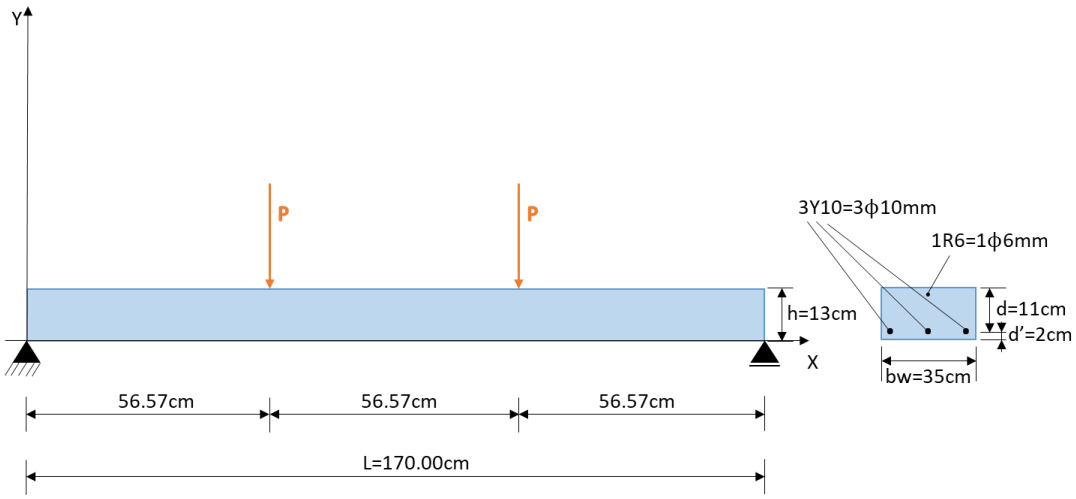

Figure 2. Beam or slab model for making graphics moment by curvature

The pit corrosion levels submitted to the beam were 6%, 8%, 9% and 14%, in relation to the mass loss of the longitudinal bars. Figure 3 represents the experimental moment curvature behavior obtained by Kearsley and Joyce [14], considering the respective level of corrosion.

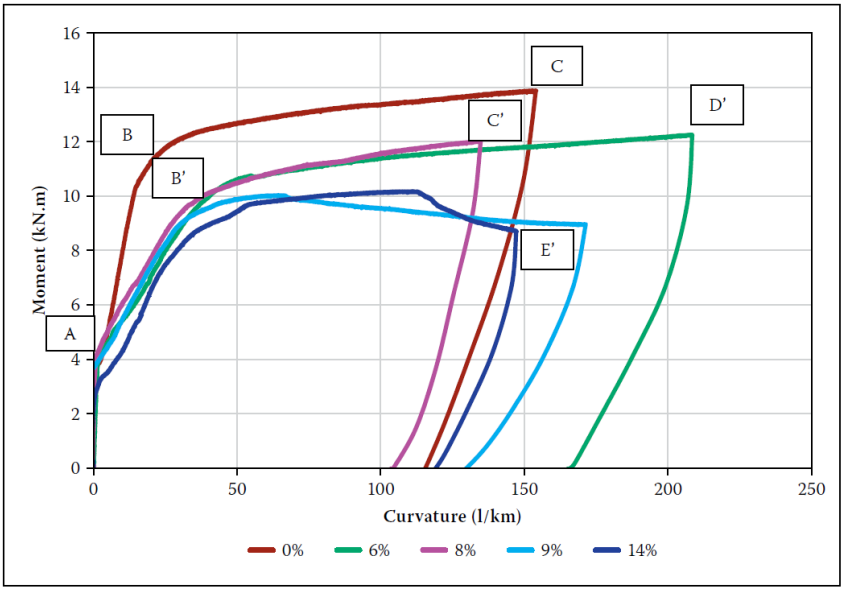

Figure 3. Graph of moment by curvature, experimental

The regions 0-A and B-C (or B'C' or B'D') are regions of sharp stiffness before the concrete crack and considerable decrease of flexural rigidity (with yielding and hardening or softening of the reinforcement), respectively. The test was completed when the hydraulic jack reached an extension of 25 mm.

Tensions and deformations in steel as a function of corrosion

As a starting point, it was necessary to know the stress function in the steel bars, which is dependent on the magnitude of the deformation and the level of corrosion of the bars. For this, the steel behavior was modeled according to experimental results obtained by Du, Clark and Chan [13]. The Figure 4 shows the experimental behavior of the force by elongation of steel bars subjected to three different pit corrosion levels (0.00%, 4.80% and 16.30%).

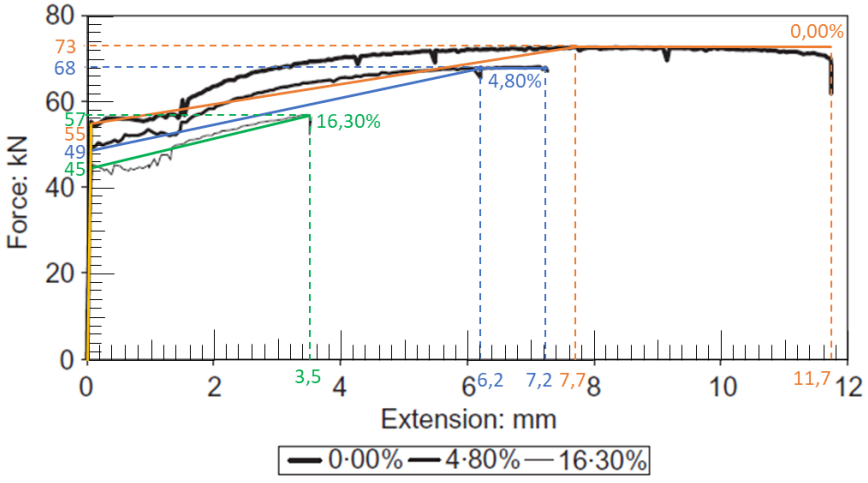

Figure 4. Graph of tensile strength by elongation obtained experimentally

According to Figure 4, there was a simplification of the graphs as verified through the straight (colored) lines. This simplification was necessary for drawing the strain graphs by deformation of the steel bars. According to Du et al. [13], the bars were tested alone, under a single tensile test, with the original diameter of the bars being 16 mm, the length of 45 cm and the modulus of elasticity of 213 GPa.

Thus, from the data of the Figure 4 and the compatibility of the input data of the works of Du et al. [13] and Kearsley and Joyce [14], relating to the respective corrosion levels (cor), the flow stress (f_y), the plastic strain at the beginning of the last stress (ε_{up}), the ultimate strain (ε_u) and the ultimate stress (f_u). This is represented in Table 3 below.

Table 3. Values of corrosion levels, stresses and strains

cor	fy (MPa)	εup	Eu	fu (MPa)
0.0000	456	0.017111	0.026	605.2364
0.0480	396.5044	0.013778	0.016	550.2511
0.1630	342.684	0.007778	0.007778	434.0664

Thus, from the organization of this table, it was possible to make four linear regressions, obtaining the functions of $f_y(cor)$, $\varepsilon_{up}(cor)$, $\varepsilon_u(cor)$ and $f_u(cor)$.

As a limitation, it should be noted that these functions are based on experiments that use data from corrosion levels ranging from 0 to 16.30%, so that it is not advisable to extrapolate this domain.

The respective equations can be verified next (Equations 13, 14, 15 and 16).

$$f_y(cor) = -653.609.cor + 444.3667 \tag{13}$$

$$\varepsilon_{up}(cor) = -0.05633.cor + 0.016851 \tag{14}$$

$$\varepsilon_u(cor) = -0.10442.cor + 0.023937 \tag{15}$$

$$f_u(cor) = -1042.8342.cor + 603.1973 \tag{16}$$

Simulation of moment by curvature plots

The initial data for creating bending moment graphs are the geometry and material parameters. These are: f_{ck} = 27.04MPa, b_w = 35 cm, h = 13cm, y_t = 6.5cm, dd = 11cm, E_s = 213GPa, f_{yk} = 456MPa, d'= 2cm, f_{ct} = 7.2MPa, E_c = 11492MPa , ε_{cu} = 0.004 and ε_{c0} = 0.002.

The Maple software was used for the modeling. Also, as input data, corrosion levels were inserted through the corrosion variables: cor = 0.00, cor = 0.06, cor = 0.08, cor = 0.09 and cor = 0.14 , observing exactly the levels of corrosion treated in the work of Kearsley and Joyce [14].

These corrosion variables were considered in calculating the stresses f_y and f_u, as already described, and also in obtaining the effective areas of steel (A_{ef}), according to Equation 17.

$$A_{ef} = (1\text{-}cor)\, A_0 \tag{17}$$

Where A_0 is the cross section area of the integral bar (cor = 0.00).

The main equation for the moment-by-curvature modeling is obtained by the sum of axial forces equal to zero and is applied to the cross section of interest. The scheme illustrated by Figure 5 shows the stress distribution, simplified, in the cross section and related forces, for the calculation stage 3.

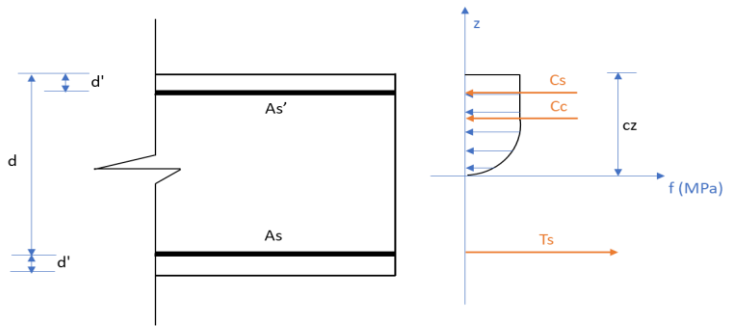

Figure 5. Equilibrium of forces in the intermediate cross section of the beam, calculation stage 3

We disregarded any effects of normal forces due to external requests (N = 0). Thus, Equation 18 was formulated below.

$$C_c + C_s = T_s \tag{18}$$

In that C_c is the compression force in the concrete, C_s is the compressive force in the steel (negative reinforcement) and T_s is the tensile force in the steel (positive reinforcement).

Thus, through a calculation routine to solve Equation 18, it was possible to simulate the moment-by-curvature graphs, as shown in Figure 6.

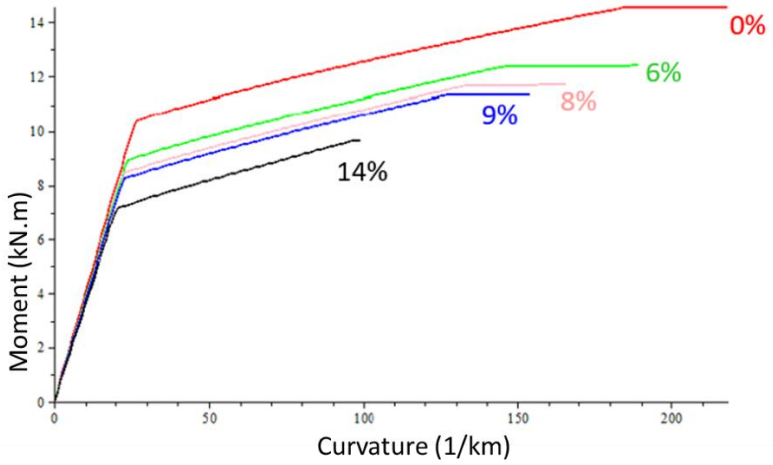

Figure 6. Results of the moment-by-curvature modeling considering corrosion effects on longitudinal reinforcement (0.00%, 6.00%, 8.00%, 9.00% and 14.00%)

Overlapping the graphs obtained with the modeling and the experimental graphs of Kearsley and Joyce [14], to better represent the approximation of the behaviors, the graphs represented by Figure 7 (includes corrosion levels: 0.00%, 6.00 % and 8.00%) and Figure 8 (includes corrosion levels: 9.00% and 14.00%).

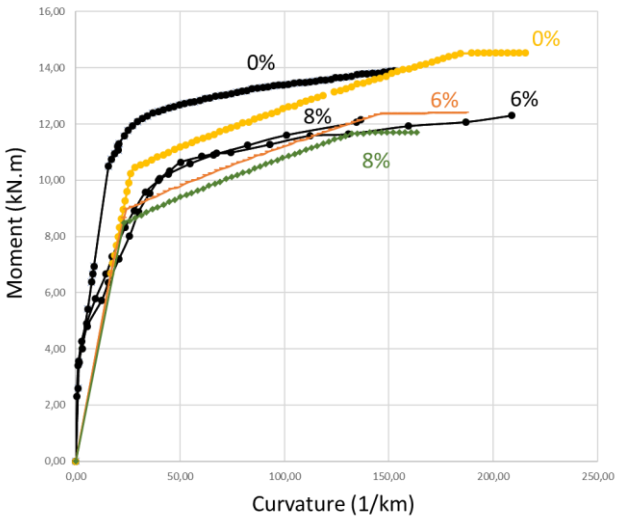

Figure 7. Overlapping of simulation and experimental graphs (0.00%, 6.00% and 8.00%)

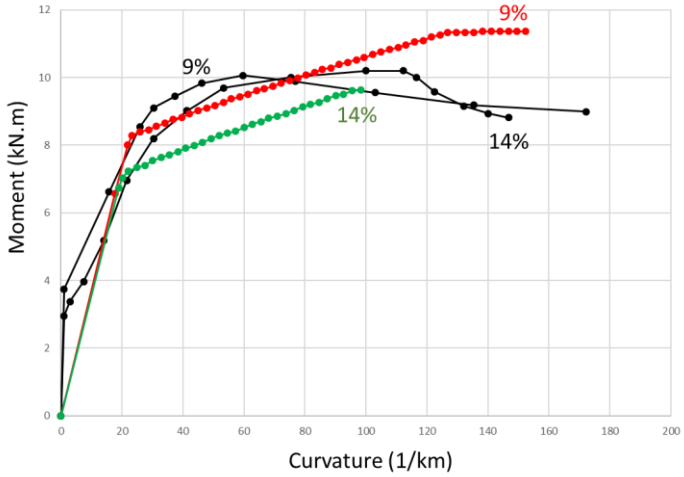

Figure 8. Overlapping of simulation and experimental graphs (9.00% and 14.00%)

The curves and colored dots refer to the results obtained with the simulation and the black curves dots are related to the experimental work of the literature.

3.2 Obtaining the values of M_{cr}, M_p, M_u e ϕ_{pu}

In this stage of the research, it was attempted to make iteration graphs that depended on the level of corrosion in the reinforcement and the normal axial force submitted to the element. These graphs serve to obtain the required input parameters of the lumped damage mechanics (R_0, q, K_0 and c) and, consequently, make possible inelastic analyzes of structures by the finite element method applied to frame elements.

In order to carry out these computations, the methodology described in section 3.1, as well as the stress and strain laws depending on the level of corrosion, were applied, which can now be applied to any percentage of corrosion, provided that less than 16% (Equations 13, 14, 15 and 16).

In this way, the graphs of the critical moment ($M_{cr}(cor, N_{cr})$) of the yielding moment ($M_p(cor, N_p)$) of the ultimate moment ($M_u(cor, N_u)$ and the final plastic rotation ($\phi_{pu}(cor, N_u)$), which depend on the level of corrosion and the respective requesting axial forces. The variables N_{cr}, N_p and N_u are, respectively, the critical, yielding and ultimate axial forces.

Figures 9 and 10 represent the simulated interaction plots.

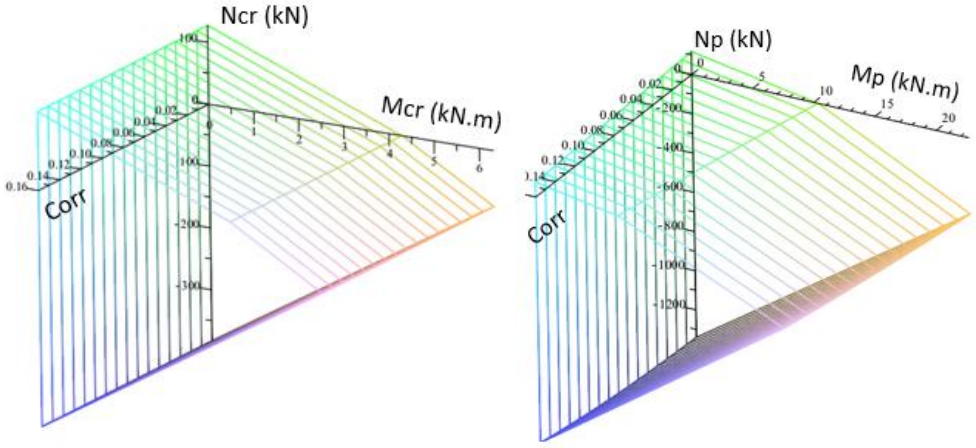

Figure 9. Iteration graphs between M_{cr}, cor and N_{cr}, and between M_p, cor and N_p

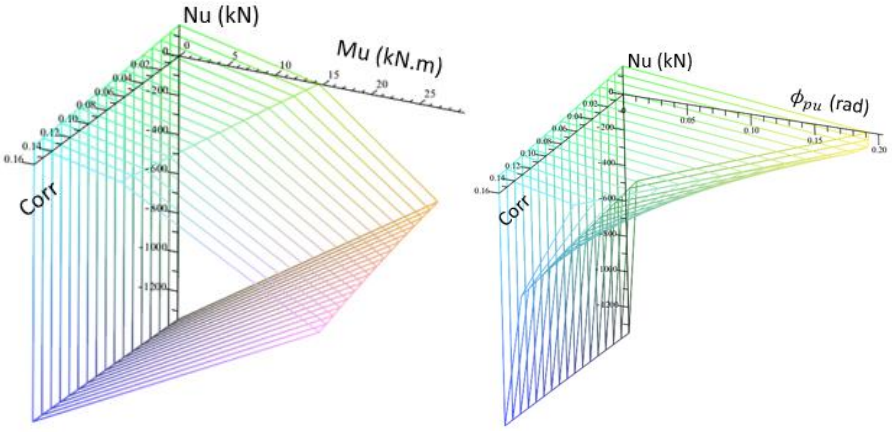

Figure 10. Iteration graphs between M_u, cor and N_u, and between ϕ_{pu}, cor and N_u

3.3 Obtaining the parameters R_0, q, K_0 e c

The procedure for obtaining these parameters was reviewed according to the work of Flórez-López et al. [10]. In addition, the corrosion of the reinforcement of the reinforced concrete structure under study was considered (Figure 2). However, theoretically, the methodology developed for confection of the model can be extended to other structures of reinforced concrete, as will be done in the next item of this work, aiming at the formalization of the proposed model.

The Figures 11 and 12 represent the iteration plots of $R_0(cor, N_{cr})$, $q(cor, N_u)$, $K_0(cor, N_p)$ and $c(cor, N_p)$.

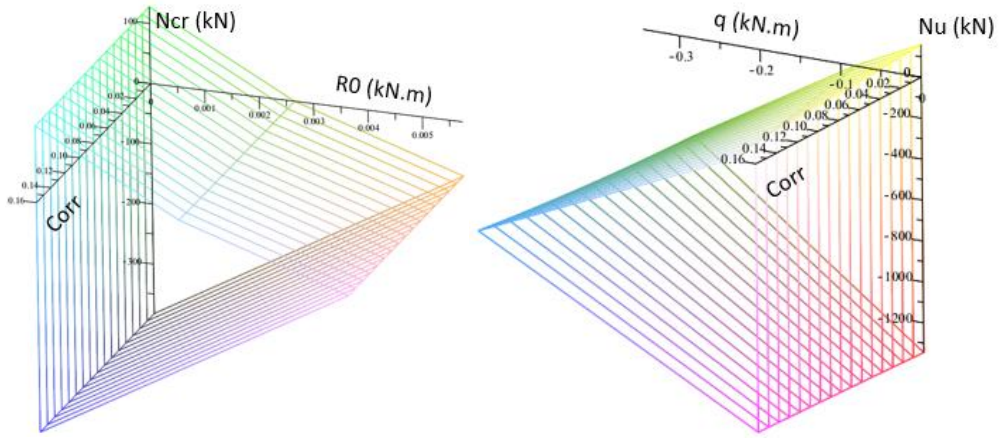

Figure 11. Iteration graphs between R_0, cor and N_{cr}, and between q, cor and N_u

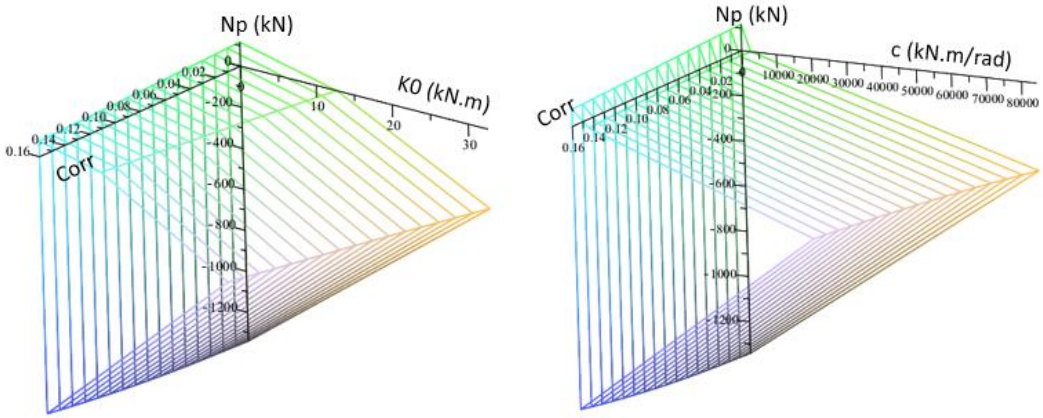

Figure 12. Iteration graphs between K_0, cor e N_p, and between c, cor e N_p

Therefore, for any level of corrosion (between 0.00% and 16.00%) and any normal force requested on the analyzed element (N_{cr}, N_p and N_u), an interpolation can be made to obtain the parameters R_0, q, K_0 and c, and perform analyzes through lumped damage mechanics.

3.4 Application of the model developed in the analysis of a reinforced concrete slab

In this section, the analysis of a reinforced concrete frame was made available in the literature. We chose a solid slab of reinforced concrete made available by Fernadez and Carranza [15]. This structure and the results of the reinforcements and the details obtained by the authors are shown in Figure 13, below.

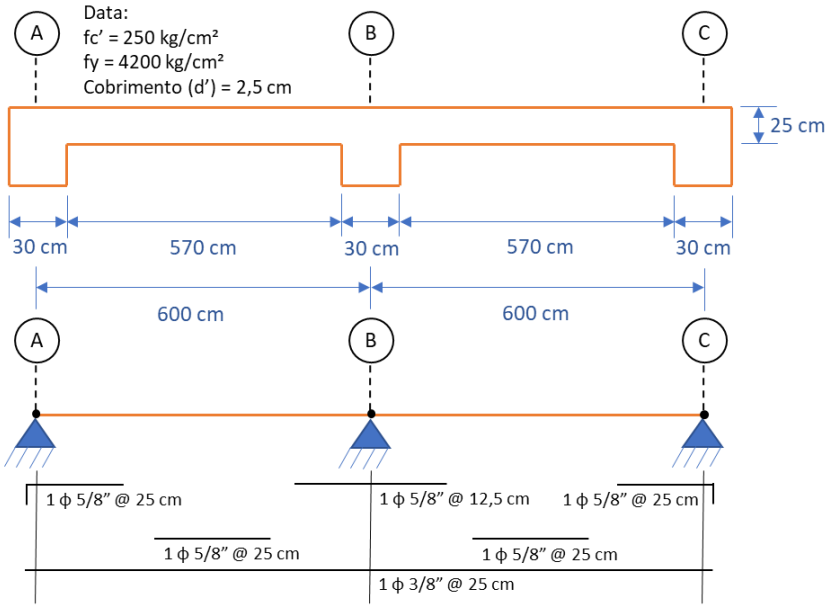

Figure 13. Slab to be analyzed

Thus, the study of the structure according to the lumped damage mechanics, which now contemplates the inelastic variables of plasticity, damage and corrosion applied to the inelastic hinges, was carried out.

The model was subjected to a permanent load (g = 12.0 kN/m) and another variable (pp = 16.0 kN/m), as shown in Figure 14. Also, under the represented structure, bending moment diagram designed at the elastic limit, treating the slab with a continuous beam of unit width (1 m).

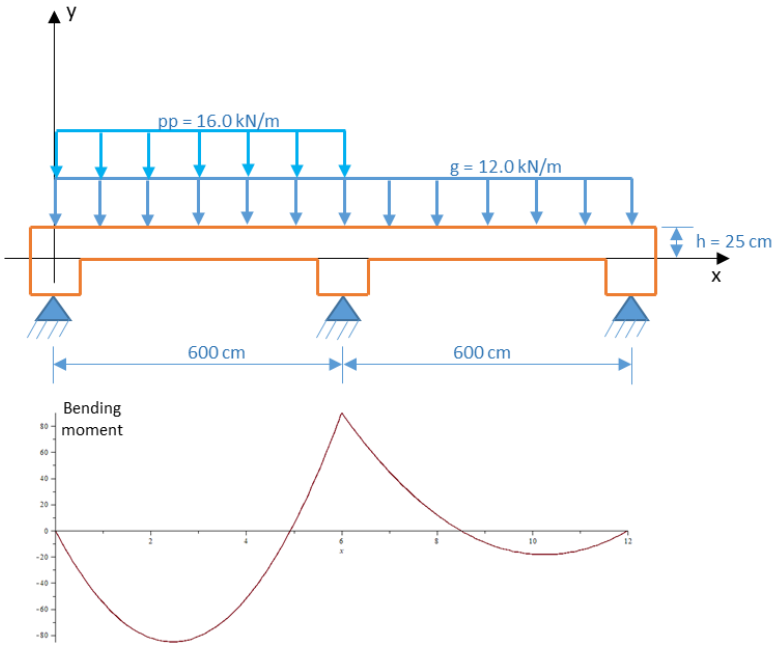

Figure 14. Static diagram of the slab and corresponding bending moment diagram

The model fitted to the analysis, by discriminating the nodes and the elements, can be verified in Figure 15. Nodes 1, 3 and 5 correspond to the slab supports and nodes 2 and 4 to positions where the values of the positive moments were maximum in the stretches, in the elastic limit.

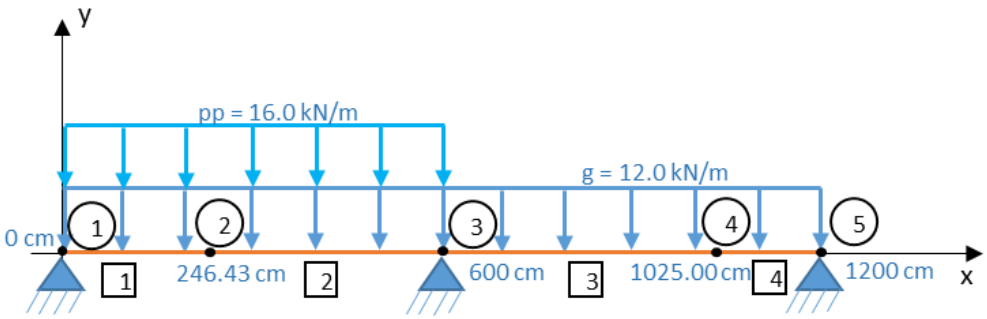

Figure 15. Model in finite elements

The processing of the structure followed the flowchart represented by Figure 16.

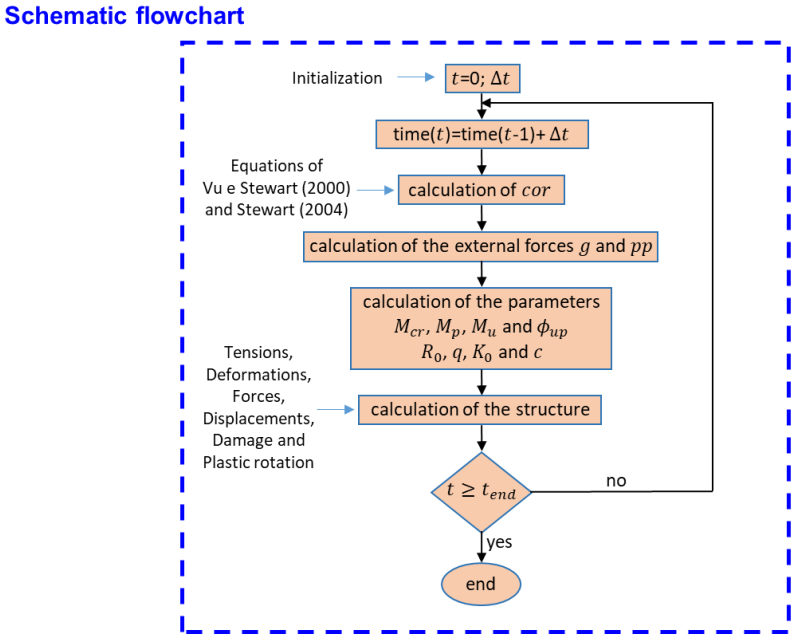

Figure 16. Schematic flow diagram of the model

For the development of the analysis, it was adopted that the corrosion begins after 20 years of the end of the construction. The evolution of corrosion in time respects the formulations developed by Vu e Stewart [11] and Stewart [12].

Simulation without considering cracking increasing corrosion

For ξ = 0, the propagation of the damage does not interfere in the evolution of the corrosion and, therefore, results of corrosion levels equivalent to those of the literature are obtained (VU and STEWART [11]; STEWART [12]), and are represented by the graph of Figure 17.

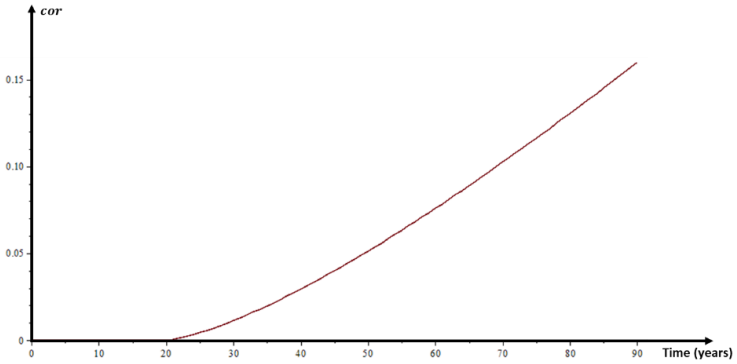

Figure 17. Behavior of corrosion in time, for $\xi = 0$

Thus, simulation of the evolution of corrosion occurs up to 90 years after the end of the construction. The final time of the analysis cannot be increased since the corrosion level would exceed 16.00% (limit level for the model).

Regarding the application of the external loads, it was standardized that the permanent load (g) would be imposed during the first day and the variable load (pp) would occur on the second day and they would remain constant afterwards.

As results of the analysis, the occurrence of damage due to the increase of the mechanical stresses (d_{12}, d_{22}, d_{23} and d_{33}) was verified. The evolutions of these lumped damages can be verified according to the graphs represented by Figure 18.

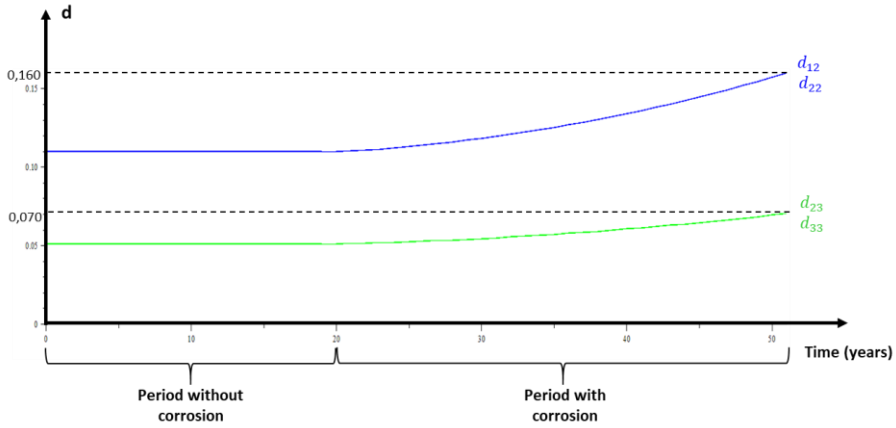

Figure 18. Damage values in time

The damaging sequence obtained with the simulation was first emerged at nodes 23 and 33, and thereafter emerged at nodes 12 and 22. This mapping of structure damaging is depicted in Figure 19, below.

Figure 19. Mapping of damage to structure

Still according to Figure 18, it can be noted that the maximum simulation time was 51 years. At that moment the first plastic hinge in the structure appears at points 12 and 22 (node 2). Thus, although external loads were already applied to the structure for a long time (51 years), corrosion was able to provoke structural instability in the form of plasticity.

Figure 20 shows the behavior of the deflection at node 2 during the simulation time. Thus, first, the emergence of the deflection with the imposition of the loading and, later, increases of the deflection because of the corrosion by pit of the reinforcement.

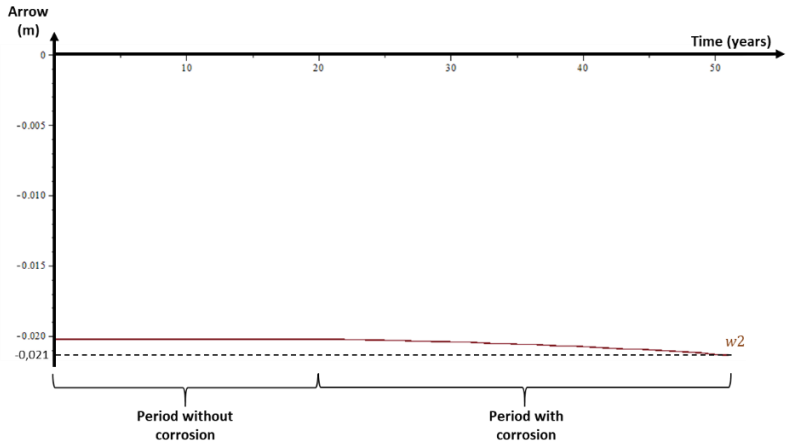

Figure 20. Arrow on node 2

Simulation considering cracking increasing corrosion

In this section, a corrosion evolution increment was added due to the presence of concrete cracking (represented by the damage variable). Now, the corrosion evolution law for any node i was formulated as follows.

$$\dot{C}_i = O_i - \xi ln^2(1 - d_i)\frac{\partial q}{\partial c_i} \tag{19}$$

As aforementioned, the dimension of the variable ξ is the inverse of the unit of energy, but there is no conviction of its magnitude, having, for that, the necessity of an experimental work aiming its determination. In this work, only a parametric study of the on influence of the new parameter is presented.

Thus, the behavior of the evolution of pit corrosion due to the cracking of the structure for values of ξ: -0.001, -0.003, -0.006 and -0.009 were considered.

For ξ = -0.001, the results of corrosion evolution were obtained, which are represented by the graph of Figure 21.

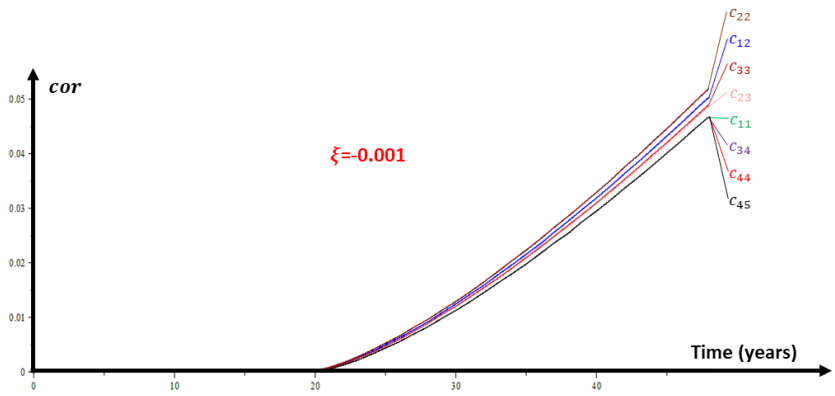

Figure 21. Behavior of corrosion in time, for ξ = -0.001

For ξ = -0.003, the results of corrosion evolution were obtained, which are represented by the graph of Figure 22.

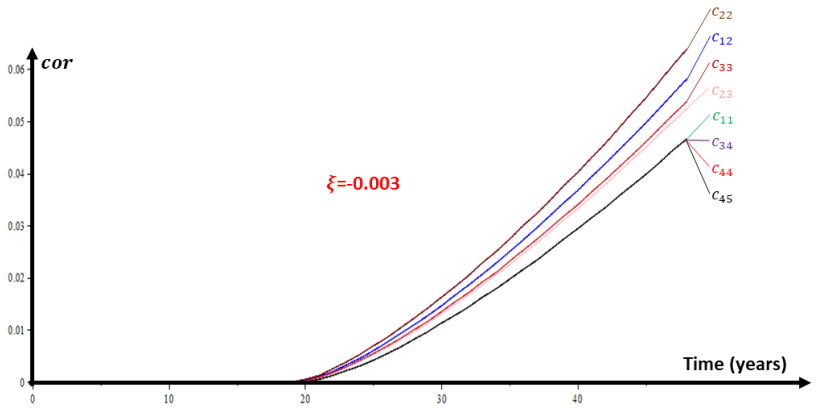

Figure 22. Behavior of corrosion in time, for ξ = -0.003

For ξ = -0.006, the results of corrosion evolution were obtained, which are represented by the graph of Figure 23.

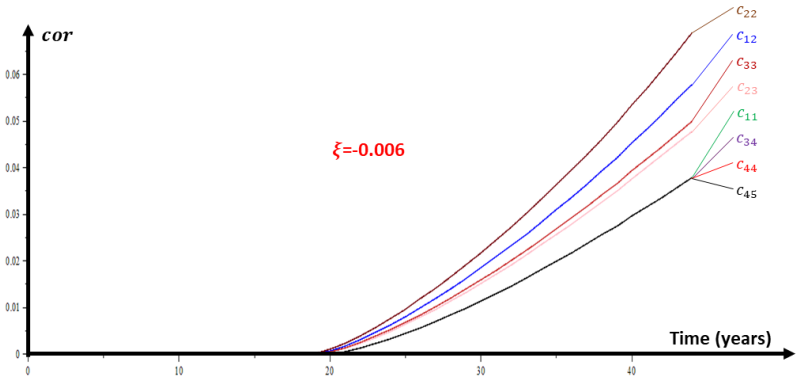

Figure 23. Behavior of corrosion in time, for ξ = -0.006

For ξ = -0.009, the results of corrosion evolution were obtained, which are represented by the graph of Figure 24.

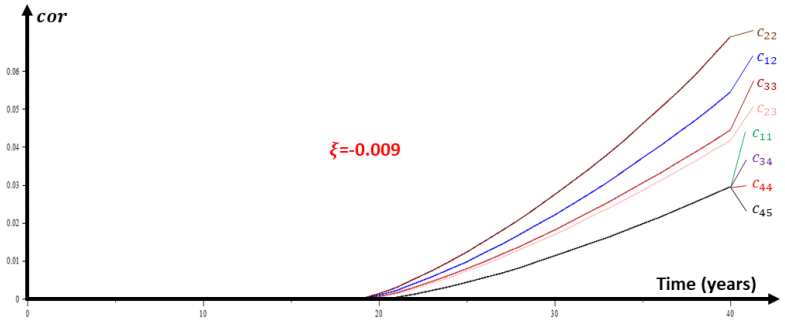

Figure 24. Behavior of corrosion in time, for ξ = -0.009

Thus, through the graphs shown in Figures 21, 22, 23 and 24, it is noted that absolute values of ξ greater than zero cause the increase of the corrosion evolution for the nodes subject to propagation of the damage, as theoretically expected, since the cracking of the concrete facilitates the penetration of aggressive agents from the medium (chloride ions, in this case).

The greater the modulus of ξ, the higher the rate of evolution of corrosion to a node where the damage is being increased. This causes the time for the appearance of the first plastic hinge to decrease and, consequently, may cause structural stability to be penalized. For example, for ξ = -0.001, the simulated time for the appearance of the first plastic hinge on the slab under analysis was 50 years, for ξ = -0.009, this time was reduced to 40 years.

Finally, by relating ξ to the deflection at node 2 of the structure, where activation of the plastic hinge occurs, a graph can be made that is represented by Figure 25. In turn, this graph can evidence the expected behavior in an experimental work, in which the deflection can be directly measured, and the associated damage can be measured through the stiffness variation method, obtaining possible values for ξ and thus validating the model experimentally.

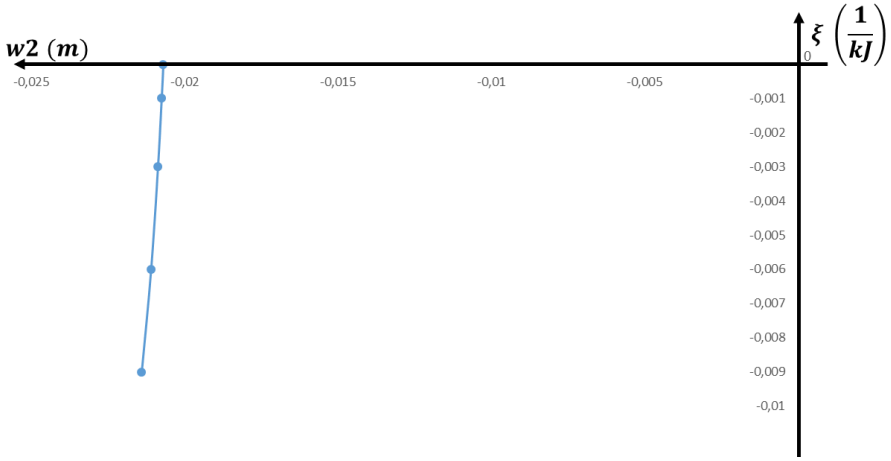

Figure 25 – Graph of ξ ($w2$) for a time of 40 years.

4 Final remarks and conclusions

It was verified in this work that lumped damage mechanics allows the direct coupling of corrosion in inelastic analyzes of current structures of reinforced concrete. This can make feasible probabilistic fault analysis through several simulation methods, such as Monte Carlo. It is worth noting that the corrosion phenomenon is not deterministic, so the proposed model may be, in the future, coupled with methods of simulation of probabilities.

The model in development could be modified to contemplate other laws of evolution of the corrosion, being thus possible to be replicated to structures subject to diverse environmental conditions. As a future route of this line of research, the possibility of working corrosion effects caused by the mechanism of carbonatation of the concrete is also investigated.

As for the analyzed example (flat slab), it was possible to verify that the evolution of the corrosion by pit causes the propagation of the damage in previously cracked hinges and the activation of plastic hinges. Consequently, this causes the penalization of the structural rigidity and the increase of the deformations and displacements of the structure, mainly, of the deflection in node 2.

In addition to simulating the effects of corrosion on structure damage, the model also allows us to take into account the corrosion evolution from concrete cracking, which results in a reduction in the time required to reach the corrosion state critical by the influence of chloride ions. Thus, for collapse mechanisms not only expected due to the part of corrosion associated with chemical forces of the medium, the model is a significant alternative for analyses of structural health diagnoses. However, as a limitation, it is necessary to perform experimental tests for the modeling of the experimental

parameter ξ.

References

[1] B. A. Shaw and R. G. Kelly. What is corrosion? *The Electrochemical Society Interface*, p. 24-26, 2006.
[2] J. M. D. Araújo. Curso de Concreto Armado, Rio Grande, v. 1, p. 1-2, 2014.
[3] R. C. Carvalho and J. R. D. Figueiredo Filho. Cálculo e detalhamento de estruturas usuais de concreto armado. 4. ed. São Carlos: EdUFSCar, 2015. p. 1-20.
[4] L. Bertolini, B. Elsener, P. Pedeferri and R. P. Polder. Transport Processes in Concrete. *Corrosion of Steel in Concrete*, WILEY-VCH Verlag GmbH & Co, p. 20-50, 2004.
[5] M. Carsana, F. Canonico and L. Bertolini. Corrosion resistance of steel embedded in sulfoaluminate-based binders. *Cement and Concrete Composites*, Milano, n. 88, p. 211-219, 2018.
[6] V. Gentil. Corrosão. 3. ed. Rio de Janeiro: *Livros Técnicos e Científicos Editora S.A.*, 1996.
[7] E. P. Figueiredo and G. Meira. Reinforcement corrosion of concrete structures. Mérida: Asociación Latinoamericana de Control de Calidad, Patología y Recuperación de la Construcción: ALCONPAT Internacional, v. 6, 2013.
[8] K. O. COELHO. Modelos numéricos aplicados à modelagem probabilística da degradação mecânica do concreto e corrosão de armaduras. Dissertação de mestrado (EESC-USP) São Carlos, 2017.
[9] R. R. Dahmer. Modelos para análise de estruturas submetidas a solicitações químico-mecânicas. Universidade Federal da Integração Latino-Americana. Foz do Iguaçu. 2018.
[10] J. Flórez-López, M. E. Marante and R. Picón. Fracture and Damage Mechanics for Structural Engineering of Frames. Hershey: IGI Global, p. 1-83. 2015.
[11] K. A. T. Vu and M. G. Stewart. Structural reliability of concrete bridges including improved chloride-induced corrosion models. *Structural Safety*, Newcastle, v. 22, p. 313-333, 2000.
[12] M. G. Stewart. Spatial variability of pitting corrosion and its influence on structural fragility and reliability of RC beams in flexure. *Structural Safety*, 2004.
[13] Y. G. Du, L. A. Clark and A. H. C. Chan. Residual capacity of corroded reinforcing bars. *Magazine of Concrete Research*, Edinburgh, v. 57, n. 3, p. 135–147, 2005.
[14] E. P. Kearsley and A. Joyce. Effect of corrosion products on bond strength and flexural behaviour of reinforced concrete slabs. *Journal of the South African Institution of Civil Engineering*, Pretoria, v. 56, n. 2, p. 21–29, 2014.
[15] E. O. B. Fernandez and S. A. D. Carranza. Concreto armado: aspectos fundamentales. 2. ed. 2013.
[16] A. T. D. Albuquerque and S. Otoch. Proposta de classificação da agressividade do ambiente na cidade de Fortaleza. *Anais do 47º Congresso Brasileiro do Concreto-CBC2005*, Fortaleza, n. 47, p. 743-748, 2005.
[17] G. M. S. ALVA and A. L. H. D. C. E. DEBS. Application of lumped dissipation model in nonlinear analysis of reinforced concrete structures. *Engineering Structures*, Santa Maria, v. 32, p. 974-981, 2010.
[18] A. M. C. Alves. Contribuição à análise da perspectiva de vida útil de estruturas em concreto face ao teor de cloreto registrado em Maceió-AL. Dissertação de mestrado, Maceió, 2007.
[19] D. L. N. D. F. Amorim, S. P. B. Proença and J. Flórez-López. A model of fracture in reinforced concrete arches based on lumped damage mechanics. *International Journal of Solids and Structures*, São Carlos, v. 50, p. 4070–4079, 2013.
[20] D. L. N. D. F. Amorim, S. P. B. Proença and J. Flórez-López. Simplified modeling of cracking in concrete: Application in tunnel linings. *Engineering Structures*, São Carlos, v. 70, p. 23–35, 2014.
[21] C. Andrade, C. Alonso and F. J. Molina. Cover cracking as a function of bar corrosion: Part I-Experimental test. *Materials and Structures*, Madrid, v. 26, p. 453-464, 1993.
[22] F. A. D. Araújo and S. P. B. Proença. Application of a lumped dissipation model to reinforced concrete structures with the consideration of residual strains and cycles of hysteresis. *Journal of mechanics of materials and structures*, v. 3, n. 5, p. 1011-1031, 2008.
[23] A. K. Chopra. Dynamics of structures: theory and applications to earthquake engineering. 4. ed. San Francisco: Prentice Hall, 2012.
[24] A. A. Cipollina, A. López-Inojosa and J. Flórez-López. A simplified damage mechanics approach to nonlinear analysis of frames. *Cumputers e Structure*, Mérida, v. 54, p. 1113-1126, 1995.

[25] K. O. COELHO, E. D. LEONEL and J. Flórez-López. Analysis of complex RC structures subjected to chemo-mechanical loadings. EASEC-15, Xi'an, p. 1-7, 2017.
[26] Y. G. Du, L. A. Clark and A. H. C. Chan. Residual capacity of corroded reinforcing bars. *Magazine of Concrete Research*, Edinburgh, v. 57, n. 3, p. 135–147, 2005.
[27] J. Flórez-López. Frame analysis and continuum damage mechanics. *European Journal of Mechanics*, Paris, v. 17, n. 2, p. 269-283, 1998.
[28] J. Lemaitre and J. L. Chaboche. Mechanics of solid materials. New York: CAMBRIDGE UNIVERSITY PRESS, p. 37-65. 1990.
[29] V. A. Lubarda. On thermodynamic potentials in linear thermoelasticity. *International Journal of Solids and Structures*, San Diego, n. 41, p. 7377–7398, 2004.
[30] M. E. Marante and J. Flórez-López. Three-dimensional analysis of reinforced concrete frames based on lumped damage mechanics. *International Journal of Solids and Structures*, Mérida, v. 40, p. 5109–5123, 2003.
[31] E. McCafferty. Introduction to Corrosion Science. New York: Springer , 2010.
[32] P. K. Mehta and P. J. M. Monteiro. Concrete: Microstructure, Properties and Materials. 3. ed. New York: McGraw-Hill, 2006.
[33] G. R. Meira and I. J. Padaratz. Efeito do distanciamento em relação ao mar na agressividade por cloretos. *Instituto Brasileiro de Concreto - 44º Congresso Brasileiro*, João Pessoa, n. 44, 2002.
[34] A. M. Neville. Propriedades do Concreto. 5. ed. São Paulo, 2016.
[35] V. T. Ngala and C. L. Page. Effects of carbonation on pore structure and diffusional properties of hydrated cement pastes. *Cement and Concrete Research*, Birmingham, v. 27, n. 7, p. 995-1007, 1997.
[36] M. Otieno, H. Beushausen and M. Alexander. Prediction of corrosion rate in RC structures - a critical review. *Modelling corroding concrete structures*, Spain, 2011.
[37] M. Otieno, H. Beushausen and M. Alexander. Prediction of corrosion rate in reinforced concrete structures – a critical review and preliminary results. *Materials and Corrosion*, Rondebosch, v. 63, n. 9, p. 777-790, 2012.
[38] V. G. Papadakis, A.P. Roumeliotis, M.N. Fardis and C.G. Vagenas. Concrete repair, rehabilitation and protection. London: E&FN Spon, 1996.
[39] J. J. D. C. Pituba. Estudo e aplicação de modelos constitutivos para o concreto fundamentados na mecânica do dano contínuo, EESC-USP (Dissertação de mestrado). São Carlos, 1998.
[40] E. Possan. Modelagem da carbonatação e previsão de vida útil de estruturas de concreto em ambiente urbano, Universidade Federal do Rio Grande do Sul - Escola de Engenharia (Tese de doutorado), Porto Alegre, p. 66, 2010.
[41] S. P. B. Proença. Fundamentos da termodinâmica dos sólidos. Apostila: introdução à mecânica do dano e fraturamento. EESC-USP, São Carlos, p. 10, 2000.
[42] J. Rajasankar, N. R. Iyer and A. M. Prasad. Modelling inelastic hinges using CDM for nonlinear analysis of reinforced concrete frame structures. *Computers and Concrete*, Chennai, v. 6, n. 4, p. 319-341, 2009.
[43] P. Schießl and S. Lay. Predictive and Optimised Life Cycle Management. New York: Taylor e Francis, 2006.
[44] M. G. Stewart, X. Wang and M. N. Nguyen. Climate change impact and risks of concrete infrastructure deterioration. *Engineering Structures*, New South Wales, v. 33, p. 1326-1337, 2011.
[45] R. A. Swalin. Thermodynamics of solids. 2. ed. Minneapolis: Wiley-VCH, 1972.
[46] H. F. W. Taylor. Cement chemistry. 2. ed. London: Thomas Telford, 1997.
[47] K. Tuutti. Corrosion of steel in concrete. stockholm: Swedish Cement and Concrete Research Institute, 1982.